Momentum entanglement and disentanglement between an atom and a photon

Rui Guo and Hong Guo*

CREAM Group, School of Electronics Engineering and Computer Science, Peking University, Beijing 100871, People's Repblic of China

(Received 28 February 2007; revised manuscript received 30 April 2007; published 18 July 2007)

With the quantum interference between two transition pathways, we demonstrate a scheme to coherently control the momentum entanglement between a single atom and a single photon. The unavoidable disentanglement is also studied from the first principle, which indicates that the stably entangled atom-photon system with superhigh degree of entanglement may be realized with this scheme under certain conditions.

DOI: 10.1103/PhysRevA.76.012112 PACS number(s): 03.65.Ud, 42.50.Vk, 32.80.Lg

I. INTRODUCTION

Atom-photon entanglement, for its fundamental importance in quantum nonlocality [1] and quantum information [2], has been extensively studied both on the discrete internal degree of freedom [3] and in the continuous momentum space [4–9]. As the continuous Hilbert space provides infinite quantum bases, it makes high degrees of entanglement possible. As in Fig. 1(a), due to the momentum conservation, a photon emitted along a single quantum path will be entangled to the recoiled atom with the degree, i.e., the Schmidt number K [10], inversely proportional to the linewidth of the transition [4]. Therefore, it is possible to produce superhigh momentum entanglement with a narrow spectral line [5,6].

A highly entangled state can also be produced with quantum interference [11]. As shown in Fig. 1(b), for a nearly degenerate three-level atom, the interference in the two-pathway spontaneous emission may strongly enhance the entanglement and make $K \propto 1/\Delta^2$ [11], where Δ is the separation between the upper levels. However, as the atomic coherence is difficult to be precisely controlled on the nearly degenerated levels, the "phase entanglement" effect [11] will make some entanglement information inaccessible for direct momentum detections in the experiments [9]. In order to obtain well detectable high momentum entanglement under realistic conditions, we propose a scheme with the configuration in Fig. 2(a). It has been known that [12,13] the interference in this two-path scattering may effectively squeeze one of the spectral lines, and we find, further, that this narrow line can also be used to produce a highly entangled state under certain conditions when the kinetic motion of the atom is taken into account. Compared to the spontaneous emission model in Fig. 1(b) [11], the proposed scheme does not need control of internal atomic coherence and the produced entanglement is completely detectable with momentum measurements [9]; also, the two upper levels can be chosen as well separated. Moreover, this scheme could be more efficient than the single-path scattering models [5,6] since the controlling light is classical and need not be far detuned.

In the following, we studied the unavoidable process of disentanglement caused by the momentum exchange with background photons in the environment. For the detectable entangled states in this and other possible schemes [4–6], we use the experimental R ratio [cf. Eq. (12)] to evaluate this process analytically. From the first principle, we obtain the master equation and the characteristic time scale for the disentanglement, which shows that the more highly entangled system is more fragile in the environment. With comparison to the entangling process, we yield an upper limit for the

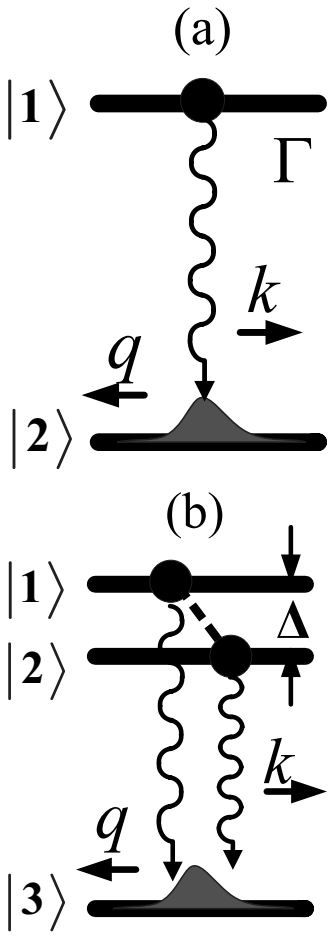

FIG. 1. (a) For the typical single-path spontaneous emission model with linewidth Γ, one has Schmidt number as $K \propto 1/\Gamma$ [4]. (b) In the two-path emission model [11], the quantum interference may enhance the entanglement as $K \propto 1/\Delta^2$, where Δ is the separation of the nearly degenerate upper levels.

*Author to whom correspondence should be addressed; hongguo@pku.edu.cn

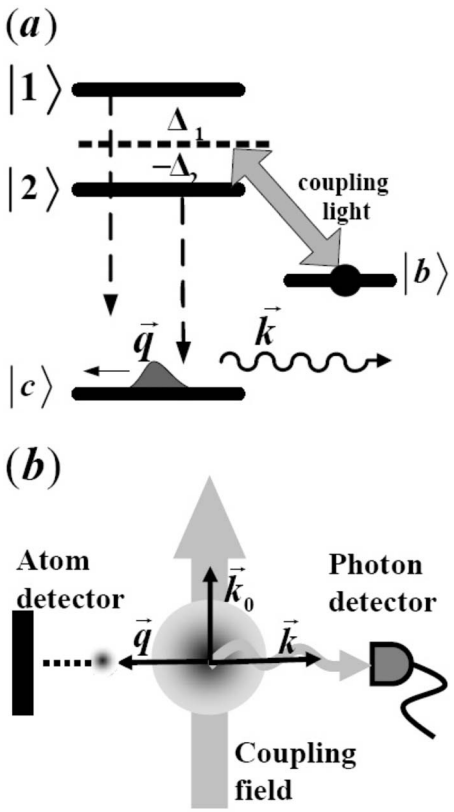

FIG. 2. (a) Atomic configuration with two well-separated upper levels. The momentum entanglement can be controlled by the classical coupling field through the interference. (b) Schematic diagram for the momentum detections. The detectors for the atom and photon are restricted in one dimension which is perpendicular to the propagation direction of the coupling light.

degree of entanglement that may be steadily produced with this scheme, which shows that, under realistic conditions [12], the robust atom-photon entangled pair can be produced with detectable superhigh degree.

II. ENTANGLEMENT GENERATION WITH QUANTUM INTERFERENCE

Concerning the kinetic degrees of freedom, the Hamiltonian for the system depicted in Fig. 2(a) can be written with the rotating wave approximation (RWA) as

$$\hat{H} = \frac{(\hbar\hat{\vec{p}})^2}{2m} + \sum_{\vec{k}} \hbar\omega_{\vec{k}}\hat{a}_{\vec{k}}^{\dagger}\hat{a}_{\vec{k}} + \sum_{j=1}^{2} \hbar\omega_{jc}\hat{\sigma}_{jj} + \hbar\omega_{bc}\hat{\sigma}_{bb} + \hbar\sum_{\vec{k}} [g_1(\vec{k})\hat{\sigma}_{c1}\hat{a}_{\vec{k}}^{\dagger}e^{-i\vec{k}\cdot\vec{r}} + g_2(\vec{k})\hat{\sigma}_{c2}\hat{a}_{\vec{k}}^{\dagger}e^{-i\vec{k}\cdot\vec{r}} + \text{H.c.}] + \hbar(\Omega_1 e^{-i\nu_0 t}e^{i\vec{k}_0\cdot\vec{r}}\hat{\sigma}_{1b} + \Omega_2 e^{-i\nu_0 t}e^{i\vec{k}_0\cdot\vec{r}}\hat{\sigma}_{2b} + \text{H.c.}), \quad (1)$$

where $\hbar\hat{\vec{p}}$ and $\vec{r}$ denote the atomic center-of-mass momentum and position operators. $\hat{\sigma}_{\alpha\beta}$ is the atomic operator $|\alpha\rangle\langle\beta|$ $(\alpha,\beta=1,2,b,c)$, and $\hat{a}_{\vec{k}}$ $(\hat{a}_{\vec{k}}^{\dagger})$ is the annihilation (creation) operator for the kth photonic mode with wave vector $\vec{k}$ and frequency $\omega_{\vec{k}}=ck$, where the polarization index is ignored for simplicity. $g_j(\vec{k})$ which we treat as constant is the coupling coefficient for the transition $|j\rangle\rightarrow|c\rangle$ and Ω_j denotes the Rabi frequency for the coupling $|j\rangle\leftrightarrow|b\rangle$ $(j=1,2)$. ν_0 and $\vec{k}_0$ denotes the frequency and the wave vector of the coupling light, and $\omega_{\alpha\beta}$ represents the difference, $\omega_{\alpha\beta}\equiv\omega_\alpha-\omega_\beta$. As the evolution is now considered in a close system, the atom-photon state can be expanded in the Schrödinger picture as

$$|\psi\rangle = \sum_{\vec{q}} [a_1(\vec{q})|\vec{q},0,1\rangle + a_2(\vec{q})|\vec{q},0,2\rangle + b(\vec{q})|\vec{q},0,b\rangle] + \sum_{\vec{q},\vec{k}} c(\vec{q},\vec{k})|\vec{q},\vec{k},c\rangle, \quad (2)$$

where the arguments in the kets denote, respectively, the wave vector of the atom, the photon, and the atomic internal state.

To eliminate the momentum exchange with the coupling light, we restrict the detections in one dimension which is perpendicular to the propagation of the coupling field, as depicted in Fig. 2(b). Then with the transformations,

$$a_1(\vec{q}) = e^{-i[T(\vec{q})+\omega_{1c}]t}A_1(\vec{q}), \quad (3)$$

$$a_2(\vec{q}) = e^{-i[T(\vec{q})+\omega_{2c}]t}A_2(\vec{q}), \quad (4)$$

$$b(\vec{q}-\vec{k}_0) = e^{-i[T(\vec{q}-\vec{k}_0)+\omega_{bc}]t}B(\vec{q}-\vec{k}_0), \quad (5)$$

$$c(\vec{q},\vec{k}) = e^{-i[T(\vec{q})+\omega_{\vec{k}}]t}C(\vec{q},\vec{k}), \quad (6)$$

where $T(\vec{p})\equiv\hbar\vec{p}^2/2m$ and $\Delta_j\equiv\omega_{jb}-\nu_0$ $(j=1,2)$, one may yield close dynamic equations from the Schrödinger equation with the Born-Markov approximation,

$$i\frac{dA_{1,2}(\vec{q})}{dt} = \Omega_{1,2}e^{i\Delta_{1,2}t}B(\vec{q}-\vec{k}_0) - \frac{i\gamma_{1,2}}{2}A_{1,2}(\vec{q}) - \frac{i\epsilon\sqrt{\gamma_1\gamma_2}}{2}A_{2,1}(\vec{q})e^{\pm i\omega_{12}t}, \quad (7)$$

$$i\frac{dB(\vec{q}-\vec{k}_0)}{dt} = \Omega_1^* e^{-i\Delta_1 t}A_1(\vec{q}) + \Omega_2^* e^{-i\Delta_2 t}A_2(\vec{q}), \quad (8)$$

$$i\frac{dC(\vec{q},\vec{k})}{dt} = g_1 e^{i[T(\vec{q})-T(\vec{q}+\vec{k})+\omega_{\vec{k}}-\omega_{1c}]t}A_1(\vec{q}+\vec{k}) + g_2 e^{i[T(\vec{q})-T(\vec{q}+\vec{k})+\omega_{\vec{k}}-\omega_{2c}]t}A_2(\vec{q}+\vec{k}), \quad (9)$$

where $\gamma_{1,2}$ denote the linewidths for the two upper levels $|1\rangle$ and $|2\rangle$; and $\epsilon\equiv\vec{\mu}_1\cdot\vec{\mu}_2/|\vec{\mu}_1|\cdot|\vec{\mu}_2|$ with $\vec{\mu}_j$ being the dipole moment for the transition $|j\rangle\rightarrow|c\rangle$ $(j=1,2)$.

Equations (7)–(9) are solved in the "dressed-state picture" in the Appendix. Due to the coupling field, the scattering along $|1\rangle$ and $|2\rangle$ can be seen as emissions from three well-separated dressed states which one may see in Fig. 3(a). It is known [13] that if dipoles of the transitions are parallel, the linewidth for the intermediate dressed state can be significantly squeezed when the field is tuned to $\Delta_1/\Delta_2\rightarrow-\gamma_1/\gamma_2$. With considerations to the kinetic degree of freedom, in the following, we will show that it is possible to produce a

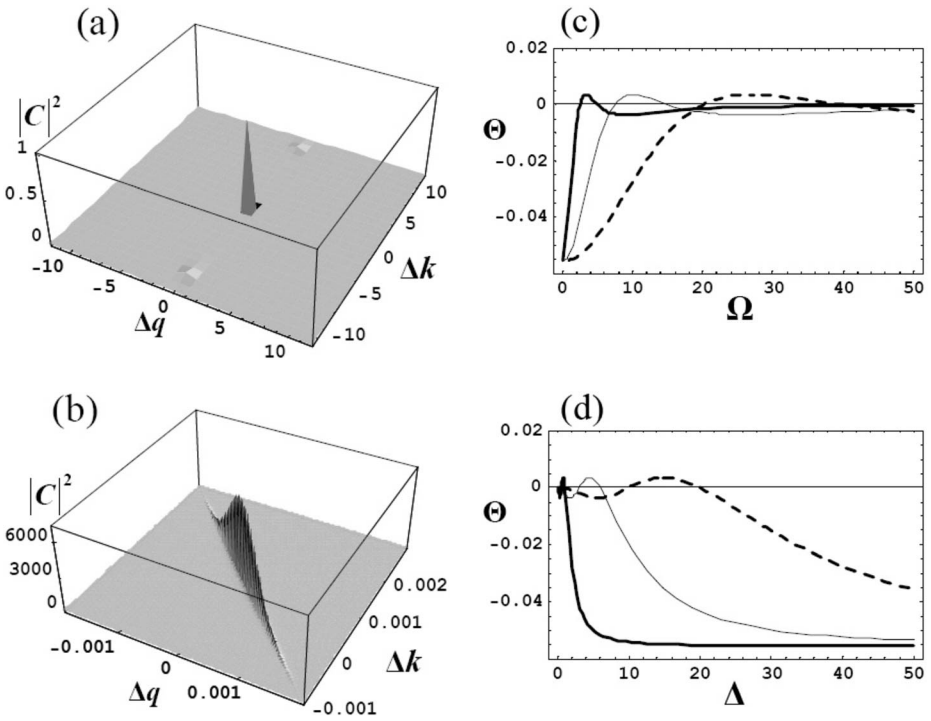

FIG. 3. (a) Distribution of $|C(\Delta q,\Delta k)|^2$ with $\gamma=1$, $\Delta=10$, $\Omega=1$, $\delta=0.01$, $\eta=0.001$. One sees that the central peak dominates the three-peaks structure which corresponds to the three dressed states. (b) Plot of the local amplification of (a), which shows that Δq and Δk are highly correlated in the central peak. (c) Plot of the function $\Theta(\Omega)$ with Δ specified as 5, 15, 40, for the bold, thin, and dashed lines, respectively. (d) Plot of $\Theta(\Delta)$ with Ω specified as 0.5, 3, 10, for the bold, thin, and dashed lines, respectively, $\gamma=1$.

highly entangled state with this interference-induced narrow line.

For the interference condition in the realistic experiment [12], we assume $\epsilon=1$, $\gamma_1=\gamma_2=\gamma$, $\Omega_1=\Omega_2=\Omega$; and $\Delta_2=-\Delta$, $\Delta_1=(1+\delta)\Delta$, where δ is a dimensionless small term controlled by the detuning of the coupling field. The atom is assumed to be excited from $|b\rangle$ with initial wave function $G(\vec{q})\propto\exp[-(\vec{q}/\delta_p)^2]$, where δ_p denotes its momentum variance. From Eqs. (7)–(9), under the weak pumping approximation (see the Appendix), we yield the steady atom-photon state in a well-known entangled form [4,5,7],

$$C(q,k,t\to\infty)\approx\chi_0\frac{\exp[-(\Delta q/\eta)^2]}{-\lambda_1/\gamma+i(\Delta q+\Delta k)},\tag{10}$$

where the complex dressed-state frequency λ_1, and the definitions of Δq, Δk, η are given in the Appendix, χ_0 is a normalization factor.

Mathematically, the entanglement of a pure bipartite system can be completely evaluated with the Schmidt number K [10], which is defined as an estimation of the number of modes that make up the Schmidt decomposition. For the state in Eq. (10), we have [4,5]

$$K\approx 1+0.28\left(\frac{\eta}{|\mathrm{Re}(\lambda_1/\gamma)|}-1\right)\approx\frac{0.28\eta}{|\Theta(\Delta/\gamma,\Omega/\gamma)|\delta^2},\tag{11}$$

with the function $\Theta(\Delta,\Omega)$ depicted in Figs. 3(c) and 3(d). From Eq. (11), one sees the entanglement is approximately inversely proportional to the dressed-state linewidth $[|\mathrm{Re}(\lambda_1)|=|\Theta(\Delta,\Omega)|\delta^2]$, which can be effectively squeezed by controlling the coupling light due to the interference in the two-pathway scattering process. We plot in Fig. 4 the degree of entanglement K with respect to the detuning $\Delta=\nu_0-\omega_{2b}$ and Rabi frequency Ω of the coupling field. From these results and Eq. (11), one then sees that the entanglement can be greatly enhanced by controlling the coupling field, and when $\nu_0\to\omega_{2b}+\omega_{12}/2$ (where $\delta\to 0$), we have $K\to\infty$.

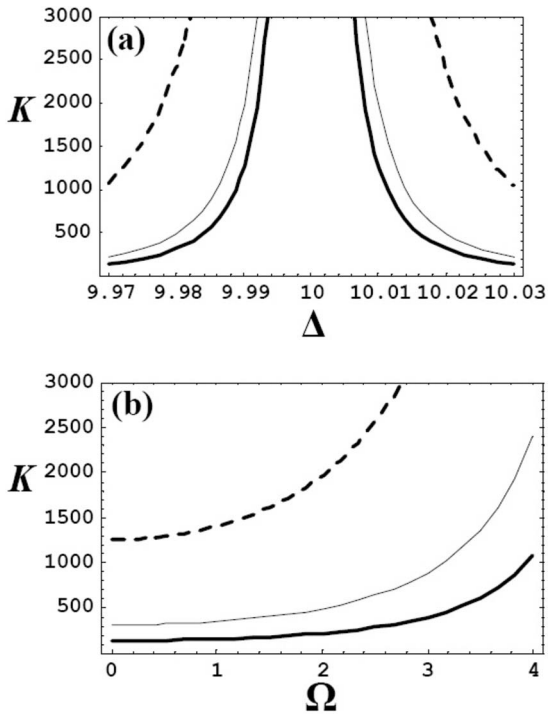

FIG. 4. Relations between the Schmidt number K and the coupling field with $\gamma=1$, $\omega_{12}=20$, $\eta=0.001$. (a) The bold, thin and dashed lines are plotted with $\Omega=0.1$, $\Omega=2$ and $\Omega=4$, respectively. (b) The bold, thin and dashed lines are plotted with $\Delta=9.97$, $\Delta=9.98$, and $\Delta=9.99$, respectively.

In the experiments [9], the degree of entanglement can be measured with the ratio (R) of the unconditional and conditional variances in the momentum detections [6–8], i.e.,

$$R \equiv \delta q^{\text{single}}/\delta q^{\text{coin}}, \tag{12}$$

$$\delta q^{\text{single}} \equiv \langle \hat{p}^2 \rangle_{\text{single}} - \langle \hat{p} \rangle^2_{\text{single}}, \tag{13}$$

$$\delta q^{\text{coin}} \equiv \langle \hat{p}^2 \rangle_{\text{coin}} - \langle \hat{p} \rangle^2_{\text{coin}}, \tag{14}$$

where δq^{single} is the variance of the atomic momentum with single-particle detection, and δq^{coin} denotes the variance obtained by coincidence detection on both the atom and the photon. From Eqs. (10) and (12), we yield

$$R \approx \frac{\eta}{1.6|\text{Re}(\lambda_1/\gamma)|} = \frac{\eta}{1.6|\Theta(\Delta/\gamma,\Omega/\gamma)|\delta^2} \approx 2.2K. \tag{15}$$

The simple linear relation between K and R in Eq. (15) indicates that the entanglement is completely detectable for the direct experiments [9] with the R ratio [6–8].

Different from the single-path scattering models [5,6], the superhigh entanglement is due to the sharp-linewidth dressed state created by the quantum interference in the two-pathway scattering. Compared with the nearly degenerate model [11] as in Fig. 1(b), this interference will not produce the "phase entanglement" and leave all the entanglement detectable in momentum measurements as we stated above. Therefore, this scheme can most probably be used to produce highly entangled atom-photon pairs in realistic applications.

III. DISENTANGLEMENT

As in the preceding section, to study the generation of momentum entanglement [4–7], it is usually convenient to assume the entangled system a close pure state system. However, in a realistic environment with $T \gg 0$ K, the interaction with environment will make the entangled system into a mixed state, and as a result, cause the disentanglement. Actually, only when the disentangling process is much slower than the generation of entanglement, the system can be approximated by a pure state. Comparing these two time scales, it is then possible to give out an upper bound for the entanglement that could be produced reliably in the environment.

Concerning the momentum entanglement, the disentanglement is caused by the momenta exchange with the environment which may be composed of background atoms and photons. Theoretically, the influence from the background atoms can be eliminated by using a high vacuum system; therefore, in order to study the unavoidable disentanglement, we can simplify the environment as a heat bath of background photons, coupled only to the entangled atom, as shown in Fig. 5(a). In order to give a general analysis for this incoherent process, the atom is simplified as a two-level system with resonant frequency ω_a, then the Hamiltonian of the total system under RWA is

$$\hat{H}_{\text{tot}} = \hat{H}_S + \hat{H}_B + \hat{H}_I, \tag{16}$$

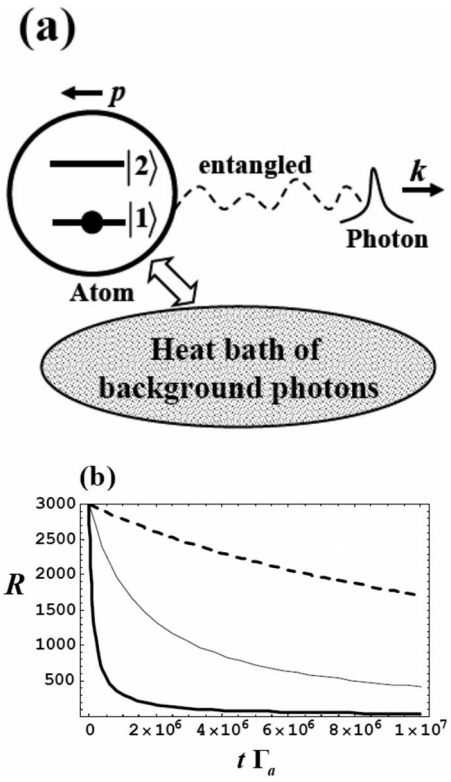

FIG. 5. (a) Schematic diagram of the disentanglement. The atom is treated as a two-level system and the environment is simplified as a heat bath of photons which is coupled to the atom through momenta exchange. (b) $R(t)$ is plotted with $\delta q_0^{\text{single}} = 16k_a^2$ and $R_0 = 3000$. The temperature of the environment is specified as $T = 300$ K for the bold line, $T = 270$ K for the thin line, and $T = 250$ K for the dashed line.

$$\hat{H}_S = \frac{(\hbar\hat{p})^2}{2m} + \hbar\omega_a\hat{\sigma}_{22} + \sum_k \hbar\omega_k\hat{b}_k^\dagger\hat{b}_k, \tag{17}$$

$$\hat{H}_B = \sum_k \hbar\omega_k\hat{a}_k^\dagger\hat{a}_k, \tag{18}$$

$$\hat{H}_I = \hbar\sum_k [g(k)\hat{\sigma}_{12}\hat{a}_k^\dagger e^{-ikr} + \text{H.c.}], \tag{19}$$

where $\hat{H}_S$, $\hat{H}_B$, and $\hat{H}_I$ denote the Hamiltonians for the system (the entangled atom-photon pair), the heat bath, and the interaction between them, respectively. $\hat{b}_k$ ($\hat{b}_k^\dagger$) is the annihilation (creation) operator for the entangled single photon in its kth mode, whereas $\hat{a}_k$ and $\hat{a}_k^\dagger$ are those for the photons in the heat bath.

It is known that the density matrix of the total system ρ_{tot} obeys the Liouville equation

$$\dot{\rho}_{\text{tot}} = \mathcal{L}_{\text{tot}}(\rho_{\text{tot}}) = (\mathcal{L}_S + \mathcal{L}_B + \mathcal{L}_I)\rho_{\text{tot}}, \tag{20}$$

where the superoperators $\mathcal{L}_{\text{tot}}$, $\mathcal{L}_S$, $\mathcal{L}_B$, and $\mathcal{L}_I$ are defined as $\mathcal{L}_{\text{tot}}(*) \equiv -\frac{i}{\hbar}[\hat{H}_{\text{tot}}, *]$, etc. In order to reveal the dynamic evolution for the entangled system, we should adiabatically

eliminate the heat-bath terms from Eq. (20) to obtain the master equation for the entangled system.

To proceed, we define the reduced density matrix for the system as $\rho \equiv \mathrm{Tr}_B(\rho_{\mathrm{tot}})$ and a "projection state" as $v \equiv \mathrm{Tr}_B(\rho_{\mathrm{tot}}) \otimes \rho_B$, where the trace "$\mathrm{Tr}_B$" is taken over the heat-bath space and ρ_B denotes the initial state of the heat bath. As the coupling is weak, from Eq. (20), we yield the equation for the projection state as

$$\dot{v} = \mathcal{L}_S v - i\rho_B \otimes \mathrm{Tr}_B\left(\mathcal{L}_I \int_0^\infty d\tau \left[\sum_k g(k)\hat{a}_k^\dagger e^{-iw_k\tau}\Lambda(\tau) + \mathrm{H.c.}, \rho \otimes \rho_B\right]\right), \tag{21}$$

where the Markov approximation and the nonrelativistic approximation $\hbar k/mc \ll 1$ are used, and $\Lambda(\tau) \equiv e^{-i\hat{H}_S\tau/\hbar}\hat{\sigma}_{12}e^{-ikr}e^{i\hat{H}_S\tau/\hbar}$.

From Eq. (21), we yield the master equation with the Lindblad form [14] as

$$\begin{aligned}\dot{\rho} = &-\frac{i}{\hbar}[\hat{H}_S,\rho] - \Gamma_a[D(\hat{\sigma}_{11}\rho + \rho\hat{\sigma}_{11}) + (1+D)(\hat{\sigma}_{22}\rho + \rho\hat{\sigma}_{22})] \\ &+ (1+D)\Gamma_a(\hat{\sigma}_{12}e^{-ik_ar}\rho\hat{\sigma}_{21}e^{ik_ar} + \hat{\sigma}_{12}e^{ik_ar}\rho\hat{\sigma}_{21}e^{-ik_ar}) \\ &+ D\Gamma_a(\hat{\sigma}_{21}e^{ik_ar}\rho\hat{\sigma}_{12}e^{-ik_ar} + \hat{\sigma}_{21}e^{-ik_ar}\rho\hat{\sigma}_{12}e^{ik_ar}),\end{aligned} \tag{22}$$

where $D \equiv \mathrm{Tr}_B(\hat{a}_{k_a}^\dagger \hat{a}_{k_a}\rho_B)$ is the average number of the resonant photons in the heat bath; the atomic linewidth is given as $\Gamma_a \equiv \Sigma_k 2\pi|g(k)|^2\delta(\omega-\omega_a)$. It is natural to assume that the heat bath is initially in the thermal equilibrium, i.e., $\rho_B = e^{-\hat{H}_B/k_BT}/\mathrm{Tr}_B(e^{-\hat{H}_B/k_BT})$, then we have $D=1/(e^{\hbar\omega_a/k_BT}-1)$, where T is the temperature of the heat bath.

The master equation, Eq. (22), describes the process of disentanglement, where the system is now in a mixed state. Mathematically, the entanglement of a mixed bipartite system can be evaluated with the "entanglement of formation" [15] which is not analytically defined. However, as the produced entanglement is completely detectable, we can use the experimental R ratio [cf. Eq. (12)] as the evaluation of entanglement, which, as will be seen in the following, gives analytical and physically reasonable results.

As in Eqs. (13) and (14), the momentum variance of the single-particle (the atom) measurement is calculated as

$$\delta q^{\mathrm{single}} = \mathrm{Tr}(\hat{p}^2\rho) - [\mathrm{Tr}(\hat{p}\rho)]^2, \tag{23}$$

while that of the coincidence measurement is

$$\delta q^{\mathrm{coin}} = \frac{\sum_{i=1}^{2}\int \mathrm{d}q q^2 \rho(q,k_0,i,q,k_0,i)}{\sum_{i=1}^{2}\int \mathrm{d}q \rho(q,k_0,i,q,k_0,i)} - \left(\frac{\sum_{i=1}^{2}\int \mathrm{d}q q \rho(q,k_0,i,q,k_0,i)}{\sum_{i=1}^{2}\int \mathrm{d}q \rho(q,k_0,i,q,k_0,i)}\right)^2, \tag{24}$$

where $\rho(q,k,i,q',k',i')$ denotes the matrix element $\langle q,k,i|\rho|q',k',i'\rangle$, and the photon is assumed to be detected with some momentum k_0.

With Eqs. (22)–(24), it is straightforward to obtain

$$R(t) = R_0 \frac{\delta q_0^{\mathrm{single}}/4Dk_a^2 + \Gamma_a t}{\delta q_0^{\mathrm{single}}/4Dk_a^2 + R_0\Gamma_a t}, \tag{25}$$

where R_0 and $\delta q_0^{\mathrm{single}}$ are defined as their initial values, $R_0 \equiv R(t=0)$ and $\delta q_0^{\mathrm{single}} \equiv \delta q^{\mathrm{single}}(t=0)$. It can be seen from Fig. 5(b) that, $R(t)$ decreases monotonously with time, therefore, the characteristic time scale Δt_{dis} for the disentanglement can be defined as $R(t=\Delta t_{\mathrm{dis}}) = \frac{1}{2}R_0$. As $R_0 \gg 1$, we yield

$$\Delta t_{\mathrm{dis}} \approx \frac{\delta q_0^{\mathrm{single}}}{4DR_0k_a^2\Gamma_a}. \tag{26}$$

From Eq. (26), one sees that the "disentangling time" Δt_{dis} is inversely proportional to the average number of the resonant photons in the heat bath $[D(\omega_a)]$. Therefore, by decreasing the temperature of the environment it is possible to significantly increase Δt_{dis} and then make the entangled system quite robust in the environment. However, as the temperature can never reach absolute zero, this kind of disentanglement is "unavoidable." Furthermore, as in Eq. (26), the disentangling time is also dependent on the initial entanglement, i.e., $\Delta t_{\mathrm{dis}} \propto 1/R_0$, which indicates that, the better entangled system is more fragile in the environment. Since $\Delta t_{\mathrm{dis}} \to 0$ when $R_0 \to \infty$, the ideal continuous EPR state [1] can never be reached in a realistic environment in this sense.

The physical meaning for the dependence on k_a and Γ_a in Eq. (26) is apparent: with larger energy and shorter lifetime for the transitions, the environment will exchange more momenta with the entangled atom per unit time, and as a result, accelerate the disentanglement. When temperature is low, the denominator in Eq. (26) has a sharp peak for the coupled frequency ω_a, which ensures the two-level approximation reasonable for our treatment.

As stated at the beginning of this section, the entanglement generated with Eqs. (11) and (15) is applicable only if the disentangling time is much longer than the time scale for producing the entanglement, i.e., $\Delta t_{\mathrm{dis}} \gg \Delta t_{\mathrm{ent}}$. Therefore, with Eqs. (26) and (A8), we yield the inequality

$$R_0 \ll 0.2\sqrt{\frac{\hbar k_{1c}\delta_p^3}{Dmk_a^2\Gamma_a}}, \tag{27}$$

which gives an upper bound for the entanglement that can be produced in the realistic environment with this scheme.

As in some reported experiments [12], the atomic configuration with SGC as in Fig. 2(a) can be realized by sodium dimers. With the experimental conditions $\gamma \sim 10^{-7}$ ω_{1c}, $\omega_{12} \sim 10\gamma$, $\Omega \sim \gamma$, when the coupling field is tuned to $\Delta \sim \omega_{12}/2 \sim 5\gamma$ with $\delta = 10^{-2}$, from Eq. (A8), we have $\Delta t_{\mathrm{ent}} \sim 1$ ms. Take the time of flight into account [5], the initial momentum variance can be prepared as $\hbar\delta_p/m = 1$ m/s, and then from Eq. (15) we obtain a superhigh degree of entanglement as $R \approx 4600$ and $K \approx 2100$. To consider

the disentanglement, we take $\omega_a = 5 \times 10^{14}$ Hz and $\Gamma_a = 10^7$ Hz for estimations. With the environment temperature $T = 150$ K, from Eq. (26), we have $D \sim 10^{-11}$ and $\Delta t_{\text{dis}} \sim 10^4$ s. One sees that the relation $\Delta t_{\text{ent}} \ll \Delta t_{\text{dis}}$ can be well fulfilled. Therefore, under these conditions, the robust highly entangled atom-photon pairs can be steadily produced in the environment. Actually, from Eq. (27), we have an upper bound as $R \ll 10^7$, which implies a strong ability of producing entanglement with this scheme. On the other hand, if the environment is at a high temperature, e.g., $T = 400$ K, the disentanglement will be strongly enhanced and we now have $\Delta t_{\text{ent}} \sim \Delta t_{\text{dis}}$. With direct detections [9], it is then possible to observe all these phenomena in experiment.

IV. CONCLUSION

In this paper, we demonstrate that for the configuration in Fig. 2(a), the interference-induced narrow spectral line [13] can be used to produce superhigh atom-photon entanglement if the atomic momentum is taken into account. By controlling the coupling field, a highly entangled state can be produced under realistic conditions. Further, we find that the interference in this model will not induce the "phase entanglement" [11] and leaves the entanglement completely detectable for the momentum measurements in experiment [9].

The disentanglement, as we studied from the first principle, will give a natural upper limit for the entanglement one may obtain with the possible schemes [4–6], since the more highly entangled state will be more fragile as seen from our analytical results. This demonstrates, from another point of view, that the ideal EPR state [1] is physically unavailable. With a low-temperature vacuum system where the momentum exchange with the environment is restricted, it is shown that a robust and highly entangled atom-photon pair can be produced with this proposed scheme. Since we analyze the two different physical processes separately and both from the first principle, most of our conclusions can directly apply to other models [4–7].

To give a more precise upper bound than Eq. (27), one must consider the generation of entanglement together with the disentanglement at the same time, which is necessary to rigorously analyze the system when $\Delta t_{\text{ent}} \sim \Delta t_{\text{dis}}$. However, this method is more complicated to be generalized and will not change our above conclusions qualitatively. We plan to give the details of this method elsewhere in a future work.

ACKNOWLEDGMENTS

This work is supported by the National Natural Science Foundation of China (Grant No. 10474004), and DAAD exchange program: D/05/06972 Projektbezogener Personenaustausch mit China (Germany/China Joint Research Program).

APPENDIX: STEADY SOLUTIONS OF EQS. (7)–(9)

The solutions of the system can be obtained by transferring the states $|1\rangle$, $|2\rangle$, $|b\rangle$ and the field into the dressed-state picture. By diagonalizing the transition matrix M,

$$M = \begin{pmatrix} \frac{\gamma_1}{2} + i\Delta_1 & \frac{\epsilon\sqrt{\gamma_1\gamma_2}}{2} & i\Omega_1 \\ \frac{\epsilon\sqrt{\gamma_1\gamma_2}}{2} & \frac{\gamma_2}{2} + i\Delta_2 & i\Omega_2 \\ i\Omega_1^* & i\Omega_2^* & 0 \end{pmatrix} \tag{A1}$$

one gets the three dressed states denoted by the eigenvectors $(\alpha_j, \beta_j, \zeta_j)^T$, and their complex frequencies λ_j $(j=1,2,3)$ with the real and imaginary parts representing the linewidths and transition frequencies, respectively. Then from Eqs. (7)–(9), the steady state solution of the entangled wave function can be written as

$$C(\vec{q}, \vec{k}, t \to \infty) = \sum_{j=1}^{3} \frac{i(g_1\alpha_j + g_2\beta_j)p_j G(\vec{q} + \vec{k} - \vec{k}_0)}{-\lambda_j + i[T(\vec{q}) - T(\vec{q} + \vec{k}) + \omega_{\vec{k}} - (\omega_{bc} + \nu_0)]}, \tag{A2}$$

where p_j is determined by the initial conditions, and when the atom is initially in $|b\rangle$, the restrictions are

$$\sum_{j=1}^{3} p_j\alpha_j = 0, \quad \sum_{j=1}^{3} p_j\beta_j = 0, \quad \sum_{j=1}^{3} p_j\zeta_j = 1. \tag{A3}$$

As the detection is restricted in one dimension, the solution can be simplified as

$$C(q,k) \propto \sum_{j=1}^{3} \frac{(g_1\alpha_j + g_2\beta_j)p_j e^{-(\Delta q/\eta)^2}}{-\lambda_j/\gamma_2 + i(\Delta q + \Delta k)} \tag{A4}$$

$$\equiv \sum_{j=1}^{3} L_j(\Delta q, \Delta k), \tag{A5}$$

where the effective wave vectors are defined as

$$\Delta q \equiv \frac{\hbar(\omega_{bc} + \nu_0)}{mc\gamma_2}\left(q - \frac{\omega_{bc} + \nu_0}{c}\right), \tag{A6}$$

$$\Delta k \equiv \frac{ck - (\omega_{bc} + \nu_0)}{\gamma_2}, \tag{A7}$$

and $\eta \equiv \hbar(\omega_{bc} + \nu_0)\delta_p/m\gamma_2 c$. We use $L_{1,2,3}(\Delta q, \Delta k)$ here to denote the three different terms that make up the summation in Eq. (A4). From Eq. (A4), it can be proven that

$$\int d\Delta q d\Delta k |L_{2,3}(\Delta q, \Delta k)|^2 = o(\Omega^2/\gamma^2) \quad \text{when } \Omega \to 0,$$

which indicates that the $L_1(\Delta q, \Delta k)$ dominates the summation when the coupling field is weak, as shown in Figs. 3(a) and 3(b); therefore, Eq. (A4) can be well approximated by the single-peak function as in Eq. (10).

To give further analysis for the entanglement, from Eq. (A1), we yield $\mathrm{Re}(\lambda_1/\gamma) \approx \Theta(\Delta/\gamma, \Omega/\gamma)\delta^2$, where the value of $\Theta(\Delta/\gamma, \Omega/\gamma)$ is of order 0.1 or smaller as shown in Figs. 3(c) and 3(d). Moreover, the time scale for producing the entanglement can be characterized as $\Delta t_{\mathrm{ent}} = 1/|\mathrm{Re}(\lambda_1)| = 1/\gamma|\Theta|\delta^2$, with Eq. (15), it may be written as

$$\Delta t_{\mathrm{ent}} \approx \frac{1.6R}{\eta\gamma}. \tag{A8}$$

[1] A. Einstein, B. Podolsky, and N. Rosen, Phys. Rev. **47**, 777 (1935); J. C. Howell, R. S. Bennink, S. J. Bentley, and R. W. Boyd, Phys. Rev. Lett. **92**, 210403 (2004).

[2] S. L. Braunstein and P. V. Loock, Rev. Mod. Phys. **77**, 513 (2005).

[3] B. B. Blinov, D. L. Moehring, L. M. Duan, and C. Monroe, Nature (London) **428**, 153 (2004); J. Volz, M. Weber, D. Schlenk, W. Rosenfeld, J. Vrana, K. Sauke, C. Kurtsiefer, and H. Weinfurter, Phys. Rev. Lett. **96**, 030404 (2006).

[4] K. W. Chan, C. K. Law, and J. H. Eberly, Phys. Rev. Lett. **88**, 100402 (2002).

[5] K. W. Chan, C. K. Law, and J. H. Eberly, Phys. Rev. A **68**, 022110 (2003); J. H. Eberly, K. W. Chan, and C. K. Law, Philos. Trans. R. Soc. London, Ser. A **361**, 1519 (2003).

[6] R. Guo and H. Guo, Phys. Rev. A **73**, 012103 (2006).

[7] M. V. Fedorov, M. A. Efremov, A. E. Kazakov, K. W. Chan, C. K. Law, and J. H. Eberly, Phys. Rev. A **72**, 032110 (2005).

[8] M. V. Fedorov, M. A. Efremov, A. E. Kazakov, K. W. Chan, C. K. Law, and J. H. Eberly, Phys. Rev. A **69**, 052117 (2004).

[9] M. D. Reid and P. D. Drummond, Phys. Rev. Lett. **60**, 2731 (1988); M. S. Chapman, T. D. Hammond, A. Lenef, J. Schmiedmayer, R. A. Rubenstein, E. Smith, and D. E. Pritchard, *ibid.* **75**, 3783 (1995); C. Kurtsiefer, O. Dross, D. Voigt, C. R. Ekstroin, T. Pfau, and J. Mlynek, Phys. Rev. A **55**, R2539 (1997).

[10] R. Grobe *et al.*, J. Phys. B **27**, L503 (1994); S. Parker, S. Bose, and M. B. Plenio, Phys. Rev. A **61**, 032305 (2000); C. K. Law, I. A. Walmsley, and J. H. Eberly, Phys. Rev. Lett. **84**, 5304 (2000); W. C. Liu, J. H. Eberly, S. L. Haan, and R. Grobe, *ibid.* **83**, 520 (1999).

[11] R. Guo and H. Guo, e-print arXiv:quant-ph/0701018v2; S. Y. Zhu, R. C. F. Chan, and C. P. Lee, Phys. Rev. A **52**, 710 (1995).

[12] H. R. Xia, C. Y. Ye, and S. Y. Zhu, Phys. Rev. Lett. **77**, 1032 (1996).

[13] S. Y. Zhu and M. O. Scully, Phys. Rev. Lett. **76**, 388 (1996).

[14] G. Lindblad, Commun. Math. Phys. **48**, 119 (1976).

[15] C. H. Bennett, D. P. DiVincenzo, J. A. Smolin, and W. K. Wootters, Phys. Rev. A **54**, 3824 (1996).